ChemComm



COMMUNICATION

View Article Online



Cite this: *Chem. Commun.*, 2018, 54, 11160

Received 19th July 2018, Accepted 10th September 2018

DOI: 10.1039/c8cc05871g

rsc.li/chemcomm

Synthesis of nanosized SAPO-34 with the assistance of bifunctional amine and seeds†

Pengfei Wu,^{ab} Miao Yang,^a Lijing Sun,^{ab} Shu Zeng,^{ab} Shutao Xu, ab Peng Tian*a and Zhongmin Liu b*a

Nanosized SAPO-34 with a tunable silica content (acidity) has been synthesized with the assistance of bifunctional amine 1-[2-(2-hydroxyethoxy)ethyl]piperazine (HEEP) or its analog 1-(2-hydroxyethyl)-piperazine (HEP), in which the piperazinyl group acting as a co-template prompts the formation of the pure CHA phase, and the hydroxyl/ether groups help inhibit the crystal growth. The resultant nanocrystallines possess a large amount of Si(4Al) species, improve transport properties as confirmed by IGA, and thus exhibit enhanced MTO catalytic performance.

SAPO-34, as one of the most important representatives of the silicoaluminophosphate molecular sieve family, has attracted considerable attention due to its superior catalytic performance in the methanol-to-olefin (MTO) reaction. The moderate acidity, special CHA structure with narrow 8-ring pore openings and large chabazite cages help the MTO reaction achieve 100% conversion and over 90% light olefin ($\overline{C_2}$ $\overline{-C_4}$) selectivity. However, the diffusion limitation of the SAPO-34 catalyst is thus accentuated which leads to a fast coke deposition and a short catalytic lifetime. It is highly desirable to shorten the diffusion route, so that the coking rate can be retarded, and the catalytic lifetime can be prolonged while maintaining the high light olefin selectivity.

Previous reports have demonstrated various strategies such as the microwave assisted method, soft/hard template method, dry gel conversion method, *etc.* to decrease the crystal size or introduce mesoporous channels for SAPO-34.^{4,5} Among them, effective methods for synthesizing SAPO-34 catalysts with good MTO catalytic performance are fewer, and in most cases the high synthesis cost and complicated procedure hinder their scale-up production. Amphiphilic organosilanes with long hydrophobic alkyl chains have been found to be effective mesoporogens to prepare hierarchical porous SAPO-34 with improved MTO catalytic performance.^{6–8}

However, it is still a big challenge to control the product silica content (acidity) in this system, because the mesoporogen is actually a part of the silica source during the crystallization. The organosilanes implanted into the SAPO-34 framework turn into silanol defects after calcination. As a result, ²⁹Si NMR reveals diverse Si environments, and the catalytic properties of hierarchical porous SAPO-34 cannot be arbitrarily judged through traditional experience. Given that the acidity is one of the important parameters determining the MTO catalytic performance of the catalyst besides mesoporosity, it is highly desirable to find silicon-free compounds for the synthesis of hierarchical/nanosized SAPO-34 catalysts.

In our previous works, a reconstruction method has been developed, which allows an easy control of the composition and porosity of the hierarchical SAPO-34.^{6,9} The crystallization process is changed by the addition of sufficient ball-milled SAPO-34 precursor, which helps to go across the nucleation step and fasten the crystallization of mesoporous SAPO-34 single crystals. Another effort is to develop a new type of multifunctional organosilane. A short-chain organosilane 3-piperazinepropylmethyldimethoxysilane has been used as a "three in one" auxiliary to achieve SAPO-34 on the nanoscale.¹⁰

In this work, we provide commercial silicon-free compounds 1-[2-(2-hydroxyethoxy)ethyl]piperazine (HEEP) and 1-(2-hydroxyethyl)piperazine (HEP) for the synthesis of nanosized SAPO-34 with excellent MTO catalytic performance. HEEP/HEP contains simultaneously piperazinyl, hydrophilic hydroxyl and/or ether groups. The molecule structures of HEEP and HEP are shown in Scheme 1. It was reported that the molecules possessing abundant hydroxyl groups may cover the crystal nucleus surface, hinder their growth and obtain nanosized crystals. ^{11,12} Meanwhile the piperazinyl group has been proved by us to be efficient to direct the formation of the CHA framework. ¹⁰ Thus, HEEP and HEP are expected to be effective for the crystallization of nano SAPO-34 and allow the easy tuning of the product Si content.

HEEP/HEP-assisted synthesis of nanosized SAPO-34 was achieved with the use of a triethylamine (TEA) template and a small amount of ball-milled SAPO-34 seeds. The resultant products were designated as SP34-HEEP-s and SP34-HEP-s, respectively. To better understand the effect of HEEP/HEP,

^a National Engineering Laboratory for Methanol to Olefins, Dalian National Laboratory for Clean Energy, Dalian Institute of Chemical Physics, Chinese Academy of Sciences, Dalian 116023, China. E-mail: tianpeng@dicp.ac.cn, liuzm@dicp.ac.cn

^b University of Chinese Academy of Sciences, Beijing 100049, P. R. China

 $[\]dagger$ Electronic supplementary information (ESI) available. See DOI: 10.1039/c8cc05871g

Communication ChemComm

Scheme 1 The molecular structures of the co-templates

contrast syntheses were conducted by using piperazine (PIP) as a co-template instead of HEEP/HEP or without any co-template. The products were named as SP34-PIP-s and SP34-C-s. In parallel, syntheses without any seed were also done. The products were designated as SP34-HEEP, SP34-HEP, SP34-PIP and SP34-C, respectively. The initial SiO₂/Al₂O₃ molar ratio for all the samples was fixed at 0.31 in order to control the product Si content at a similar level. Their corresponding product phases and compositions are listed in Table 1.

The XRD patterns of the as-synthesized samples are displayed in Fig. 1. For the samples directed by TEA (SP34-C and SP34-C-s), peaks at 16.9 and 21.3 2θ degrees appeared (labeled with asterisks), suggesting the presence of the SAPO-34/18 intergrowth. 13,14 Upon the addition of PIP or its derivatives (HEEP and HEP), the SAPO-34/18 intergrowth phase was inhibited, which gave a typical CHA X-ray diffraction pattern. The results indicate that all three compounds containing piperazine groups facilitate the achievement of the pure CHA phase. This is important for the catalysts' MTO performance because the appearance of the intergrowth will decrease the selectivity to $C_2^{-} + C_3^{-}$. ¹⁰ SEM images show the morphology of the products. The crystal sizes are quite different depending on the templates used. As seen in Fig. S1 (ESI†), the product presents rhombohedral crystals of about 5 µm in size when only TEA is used, and the crystals grow even bigger when PIP derivatives are added. Twinning crystals are the main products when HEEP or HEP was used together with TEA in comparison to the individual crystals obtained from the single TEA, and TEA plus PIP systems. When 5% seeds were introduced, the crystal size decreases sharply. Interestingly, the samples directed by TEA (Fig. 2a) and TEA + PIP (Fig. 2b) show uniform cubic morphology with particle sizes of about 1 µm, implying that the small molecule PIP has little effect on the product morphology. Surprisingly, SP34-HEEP-s (Fig. 2d) and SP34-HEP-s (Fig. 2c) presented approximately cubic morphology with a rough surface, and the primary particle sizes were about 150 and 400 nm, respectively. The particle size distributions of the samples were also

Table 1 Synthesis conditions, product composition and crystalline phase^a

Sample	R	Seed (%)	Product composition	Crystalline phase
SP34-HEEP-s	HEEP	5	Si _{0.089} Al _{0.485} P _{0.426} O ₂	SAPO-34
SP34-HEP-s	HEP	5	$Si_{0.086}Al_{0.520}P_{0.394}O_2$	SAPO-34
SP34-PIP-s	PIP	5	$Si_{0.085}Al_{0.470}P_{0.445}O_2$	SAPO-34
SP34-HEEP	HEEP	_	$Si_{0.084}Al_{0.486}P_{0.430}O_2$	SAPO-34
SP34-HEP	HEP	_	$Si_{0.084}Al_{0.487}P_{0.429}O_2$	SAPO-34
SP34-PIP	PIP	_	$Si_{0.084}Al_{0.475}P_{0.442}O_2$	SAPO-34
$SP34-C-s^b$	_	5	$Si_{0.089}Al_{0.483}P_{0.428}O_2$	SAPO-34/18
$SP34-C^b$	_		$Si_{0.086}Al_{0.484}P_{0.430}O_2$	SAPO-34/18

 $[^]a$ The initial gel molar composition: R/TEA/Al₂O₃/P₂O₅/TEOS/H₂O = 1.5/4.5/1.0/1.0/0.31/100 (200 $^\circ$ C, 24 h). b Pseudoboehmite used as an Al source and alkaline silica sol as a Si source. The initial gel molar composition: $TEA/Al_2O_3/P_2O_5/SiO_2/H_2O = 3.0/1.0/1.0/0.4/50$ (200 °C, 24 h).

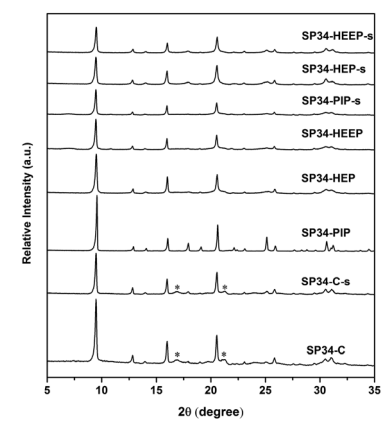


Fig. 1 XRD patterns of the as-synthesized samples. Asterisks indicate the AEI phase

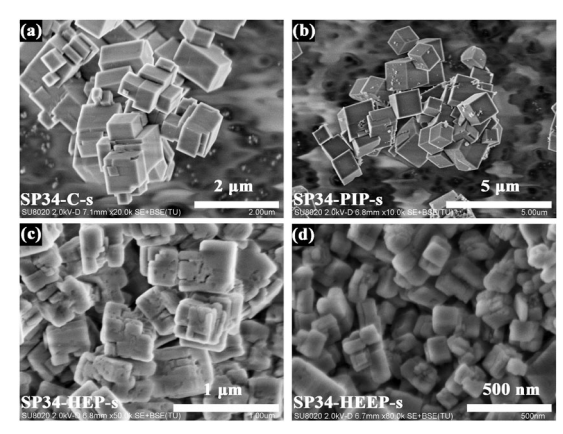


Fig. 2 SEM images of the calcined SP34-C-s (a), SP34-PIP-s (b), SP34-HEP-s (c), and SP34-HEEP-s (d).

measured by DLS (Fig. S2, ESI†), which give average particle sizes of 190 and 499 nm for SP34-HEEP-s and SP34-HEP-s, respectively. The above results suggest that the addition of HEEP and HEP can decrease the particle size heavily under the assistance of the seeds.

N₂ adsorption-desorption isotherms of SP34-HEEP-s and SP34-HEP-s are depicted in Fig. S3 (ESI†), and their textural properties are given in Table S1 (ESI†). Small hysteresis loops exist in the region $P/P_0 > 0.7$ for both samples, ascribed to the inter-crystal pores of nanoparticles. The samples SP34-HEEP-s and SP34-HEP-s exhibit increased external surface areas (35 m² g⁻¹ and 33 m² g⁻¹) and higher mesopore volumes (0.12 cm³ g⁻¹ and 0.09 cm³ g⁻¹) than those of micron-sized analogs. These characteristics would be beneficial for the diffusion of the product molecules so that the coking rate might be retarded during the MTO reaction.

Solid-state ²⁹Si and ¹³C NMR spectra were collected to investigate the atomic chemical environments and the status of the template in the samples. The ²⁹Si MAS NMR spectra are shown in Fig. 3(a). The sharp signals centered at -92 ppm are attributed to the isolated Si(OAl)₄ environment. It has been conclusively shown that the Si(OAl)₄ species provide moderate acidic sites, which are beneficial for the MTO reaction.^{3,15} The ¹³C MAS NMR results are given in Fig. 3(b). Similar spectra are observed for SP34-C,

ChemComm

(a)

-92 ppm

-92 ppm

SP34-HEEP-4

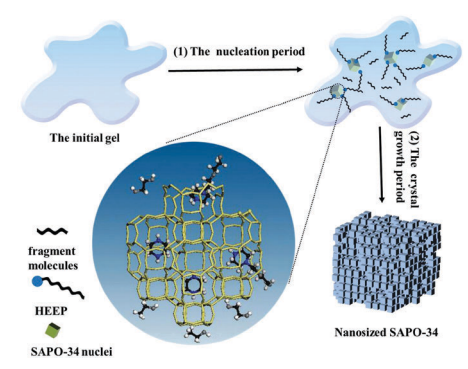
SP34-HEE

Fig. 3 $\,^{29}$ Si MAS NMR spectra (a) and 13 C MAS NMR spectra (b) of the assynthesized samples.

SP34-HEEP-s and SP34-HEP-s. The signals at 48 and 9 ppm can be related to the -CH2- and -CH3 groups of the TEA template, respectively.¹⁶ However, if only TEA exists in the sample, the peak areas of the two signals should be around 1:1, as seen in the 13C MAS NMR spectrum of SP34-C. The quite different peak areas of the two peaks for SP34-HEEP-s and SP34-HEP-s suggest the coexistence of other organics. ¹³C NMR spectra of pure chemicals of HEEP and HEP were therefore measured, which show that both chemicals have a strong signal at around 45 ppm attributed to the C atoms belonging to piperazine group (Fig. S4, ESI†). It is thus believed that the stronger signal at 48 ppm for SP34-HEP-s and SP34-HEP-s should be contributed by a piperazine like compound. Given the absence of other 13C signals in Fig. 3b, it is speculated that the coexisting template in SP34-HEEP-s and SP34-HEP-s should be PIP resulting from the decomposition of HEEP and HEP. 10 The molar ratio of PIP to TEA was calculated to be about 1.22 for SP34-HEEP-s and 0.75 for SP34-HEP-s according to peak area. Compared with the dosage of R/TEA = 0.33 (R = HEEP and HEP) in the initial gel, it is believed that PIP has a stronger structural directing ability to the CHA structure than TEA, which enters more to suppress the formation of SAPO-34/18 intergrowth. TG analyses were carried out to evaluate the total amount of organic species. The weight losses of SP34-HEEP-s and SP34-HEP-s are obviously higher than that of SP34-C, as shown in Fig. S5 and Table S2 (ESI†).

If both HEEP and HEP decompose to PIP during the reaction, why are the crystal sizes of SAPO-34 products quite smaller than those directly obtained from the PIP system? In order to clarify the role of HEEP and HEP, a possible reaction status was simulated by adding a certain amount of alcohol into the synthetic system of SP34-PIP-s. Ethanol, ethylene glycol and 2-ethoxyethanol were added separately which were the probable fragment molecules generated by the decomposition of HEP/HEEP. The synthetic results are listed in the ESI.† As seen in Fig. S6 (ESI†), the obtained samples were non-uniform and the particle sizes were even larger than SP34-PIP-s. It is thus concluded that HEP/HEEP played a non-substitutable role in the formation of nanosized SAPO-34, though they decomposed during the reaction.

Based on the above experimental results and analyses, a possible crystallization process is proposed and illustrated in Scheme 2 by taking SP34-HEEP-s as an example. The crystallization of SAPO-34 normally begins with a nucleation step which is followed by a rapid crystal growth period. The nucleation is speeded up under the assistance of SAPO-34 seeds. Because HEEP contains both piperazinyl and hydroxy groups simultaneously, it could have strong interactions



Scheme 2 Schematic of the process for the formation of nanosized SP34-HEEP-s. TEA molecules in the structures are omitted for clarity.

with the seeds and inorganic source. The AlO_4 , PO_4 and SiO_4 species surround the piperazinyl group to construct CHA cages, while the hydrophilic hydroxyethoxyethyl tail hinders the growth of SAPO-34. Thanks to the increased nucleation speed by the seeds, HEEP can play an effective role on time before its decomposition. Otherwise, it will take a long time to yield enough nuclei from the seed-deficient gels, and substantially all the metastable HEEP molecules decompose to PIP during the nucleation period. Eventually, micrometer-sized SAPO-34 was directed by PIP and TEA as co-templates.

The MTO catalytic properties of the samples with different particle sizes were evaluated in a fixed-bed reactor at 450 °C with a methanol WHSV of 2 h⁻¹. The detailed results are given in Fig. 4(a), Table 2 and Table S3 (ESI†). As expected, the SP34-HEEP-s with minimum particle size exhibit the longest catalytic lifetime of 446 min and 84.45% high ethylene plus propylene selectivity. The lifespan is over 2-fold improved compared to that of the conventional SP34-C (208 min). The low coke deposition rate and high coke content should stem from the nanoscale crystal size which benefits the diffusion of products and increases the utilization of the active centers of SAPO-34 crystals. Notably, SP34-HEEP-s and SP34-HEP-s have even longer lifetimes than that of our previously reported nanoaggregate sample synthesized with the assistance of organosilane PZMPS (SP34-PZPMS, Si_{0.087}Al_{0.502}P_{0.411}O₂, from ref. 10), though SP34-PZPMS has similar primary crystal size to SP34-HEEP-s (Fig. S7, ESI†).

The transport properties of the representative SAPO-34 catalysts were consequently evaluated by using an intelligent gravimetric analyzer (IGA). Propylene, one of the dominant products of the MTO reaction, was used as the probe molecule. As shown in the

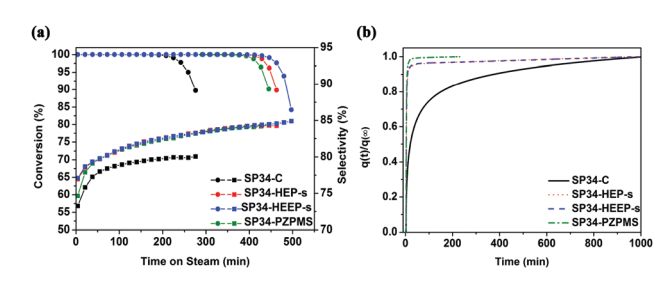


Fig. 4 (a) Methanol conversion (circular) and ($C_2H_4 + C_3H_6$) selectivity (quadrate) variation with time-on-stream over samples. Experimental conditions: WHSV = 2 h⁻¹, T = 450 °C, catalyst weight = 300 mg. (b) propylene uptake curves of the samples.

Communication ChemComm

Table 2 Lifetime^a and product distribution^b of samples in the MTO reaction (WHSV = 2 h⁻¹, T = 450 °C), and calculated values of the inverse of the diffusion time constant (D/L^2)

Sample	Lifetime (min)	$\mathrm{C}_{2}^{=}\left(\% ight)$	$C_3^{=}$ (%)	$C_2^{=} + C_3^{=}$ (%)	Coke content c (%, g g_{cat}^{-1})	$R_{\rm coke}^{c} ({\rm mg \ min}^{-1})$	D/L^2 (s ⁻¹)
SP34-HEEP-s	446	50.83	33.62	84.45	27.81	0.062	8.36×10^{-2}
SP34-HEP-s	412	51.06	33.53	84.59	25.73	0.063	3.44×10^{-2}
SP34-PIP-s	242	51.26	34.01	85.27	19.05	0.079	_
SP34-C-s	327	48.01	33.73	81.75	23.89	0.073	
SP34-C	208	43.25	37.17	80.42	20.65	0.099	1.15×10^{-3}
SP34-PZPMS ^d	376	50.00	33.65	83.65	25.19	0.064	1.08×10^{-1}

^a Catalyst lifetime is defined as the reaction duration with >99% methanol conversion. ^b The highest selectivity of $C_2^{=}$ and $C_3^{=}$ under >99% methanol conversion. Centermined using a TG and DTA analyzer up to 800 Centermined after the MTO reaction. From our previous work (ref. 10)

uptake curves of Fig. 4b, the propylene uptakes in the nanocrystals of SP34-HEEP-s and SP34-HEP-s are obviously much faster. It takes less than 9 min for the uptake to increase from 0 to 90%. Comparatively, the bulk SP34-C sample requires 372 min to achieve a similar uptake of 90%. Quantification of the diffusion properties was performed using Fick's second law (eqn (S1), ESI†). 17,18 Fig. S8 (ESI†) shows a linear relationship between $q(t)/q(\infty)$ and $t^{1/2}$, and the values of the inverse of the diffusion time constant (D/L^2) could be calculated from the slopes, which represent the mass transfer properties of the samples. As shown in Table 2, SP34-PZPMS has the largest D/L^2 value of 1.08×10^{-1} , while SP34-C has the minimum value of 1.15×10^{-3} . The D/L^2 values increase obviously with decreasing particle size of the samples, which implies that the gas phase product diffusion through the SP34-PZPMS, SP34-HEEP-s and SP34-HEP-s particles can be more effective than through SP34-C, which alleviates the formation of bulk coke species and facilitates the achievement of longer catalytic lifetimes. On the other hand, although SP34-PZPMS exhibits the shortest adsorption equilibrium time and the highest D/L^2 value, it exhibits a shorter catalytic lifetime and slightly worse light olefin selectivity than those of SP34-HEP-s/SP34-HEP-s. We speculate that the result should be due to the difference in the acidity of the catalysts.

As seen from the NH3-TPD results (Fig. S9, ESI†), SP34-PZPMS contains a smaller acid amount than SP34-HEEP-s and SP34-HEP-s, although their Si contents are comparable. The most likely cause of the decline in acid density for SP34-PZPMS is the introduction of organosilane, which generates Si-OH species in the calcined framework after the removal of organics. To confirm this speculation, solid-state ²⁹Si CP MAS NMR spectra were measured for the calcined SP34-PZPMS and SP34-HEEP-s. As shown in Fig. S10 (ESI†), the obvious shoulder peak at around -83 ppm of the calcined SP34-PZPMS could be attributed to the $Si(OAI)_n(OH)_{4-n}$ (n = 1 and 2) species.¹⁹ These defect sites are useless (maybe harmful) for the MTO reaction.²⁰ Thus, it is concluded that the longer lifetime on SP34-HEP-s and SP34-HEP-s than on SP34-PZPMS should result from the larger amount of single Si(4Al) environments, which provides more active sites with medium acidity for the reaction and contributes to the higher tolerance of the materials to the coke deposition.

In summary, by using the bifunctional amine HEEP/HEP together with a microporous template TEA, nanosized SAPO-34 was successfully synthesized. The pure CHA structure, good diffusion ability and large amount of Si(4Al) environment ensure that the catalyst exhibits an excellent MTO catalytic performance. In the future, more multifunctional amines are expected to be developed for the synthesis of hierarchical/ nanosized SAPO catalysts with high efficiency.

This work was supported by the National Natural Science Foundation of China (21476228 and 21676262) and the Key Research Program of Frontier Sciences, CAS (QYZDB-SSW-JSC040).

Conflicts of interest

There are no conflicts to declare.

Notes and references

- 1 D. Chen, K. Moljord and A. Holmen, Microporous Mesoporous Mater., 2012, 164, 239-250.
- 2 M. Dusselier and M. E. Davis, Chem. Rev., 2018, 118, 5265-5329.
- 3 P. Tian, Y. Wei, M. Ye and Z. Liu, ACS Catal., 2015, 5, 1922-1938.
- 4 Q. Sun, Z. Xie and J. Yu, Natl. Sci. Rev., 2017, nwx103, 1-17.
- 5 J. Zhong, J. Han, Y. Wei, P. Tian, X. Guo, C. Song and Z. Liu, Catal. Sci. Technol., 2017, 7, 4905-4923.
- 6 C. Wang, M. Yang, M. Li, S. Xu, Y. Yang, P. Tian and Z. Liu, Chem. Commun., 2016, 52, 6463-6466.
- 7 C. Wang, M. Yang, P. Tian, S. Xu, Y. Yang, D. Wang, Y. Yuan and Z. Liu, J. Mater. Chem. A, 2015, 3, 5608-5616.
- 8 Q. Sun, N. Wang, D. Xi, M. Yang and J. Yu, Chem. Commun., 2014, 50, 6502-6505.
- 9 M. Yang, P. Tian, C. Wang, Y. Yuan, Y. Yang, S. Xu, Y. He and Z. Liu, Chem. Commun., 2014, 50, 1845-1847.
- 10 P. Wu, M. Yang, W. Zhang, S. Xu, P. Guo, P. Tian and Z. Liu, Chem. Commun., 2017, 53, 4985-4988.
- 11 D. Jin, Z. Liu, J. Zheng, W. Hua, J. Chen, K. Zhu and X. Zhou, RSC Adv., 2016, 6, 32523-32533.
- 12 C. Zhang, X. Lu and T. Wang, J. Energy Chem., 2015, 24, 401-406.
- 13 R. L. Smith, S. Svelle, P. del Campo, T. Fuglerud, B. Arstad, A. Lind, S. Chavan, M. P. Attfield, D. Akporiaye and M. W. Anderson, Appl. Catal., A, 2015, 505, 1-7.
- 14 B. Gao, D. Fan, L. Sun, H. An, F. Fan, S. Xu, P. Tian and Z. Liu, Microporous Mesoporous Mater., 2017, 248, 204-213.
- 15 L. Xu, A. Du, Y. Wei, S. Meng, Y. He, Y. Wang, Z. Yu, X. Zhang and Z. Liu, Chin. J. Catal., 2008, 29, 727-732.
- 16 D. Wang, M. Yang, W. Zhang, D. Fan, P. Tian and Z. Liu, CrystEng-Comm, 2016, 18, 1000-1008.
- 17 A. R. Teixeira, X. Qi, C.-C. Chang, W. Fan, W. C. Conner and P. J. Dauenhauer, J. Phys. Chem. C, 2014, 118, 22166-22180.
- 18 D. Jin, G. Ye, J. Zheng, W. Yang, K. Zhu, M.-O. Coppens and X. Zhou, ACS Catal., 2017, 7, 5887-5902.
- 19 Z. Xue, J. Ma, W. Hao, X. Bai, Y. Kang, J. Liu and R. Li, J. Mater. Chem., 2012, 22, 2532-2538.
- 20 I. Yarulina, A. Dikhtiarenko, F. Kapteijn and J. Gascon, Catal. Sci. Technol., 2017, 7, 300-309.